

RECONSTRUCTION OF G^1 SURFACES WITH BIQUARTIC PATCHES FOR HP FE SIMULATIONS

Dong Xue¹

Leszek Demkowicz²

Chandrajit Bajaj³

¹*Department of Engineering Mechanics, University of Texas at Austin, TX, 78712
cynthia@ices.utexas.edu*

²*Institute of Computational Engineering and Science, University of Texas at Austin, TX, 78712
leszek@ices.utexas.edu*

³*The Center for Computational Visualization, University of Texas at Austin, TX, 78712
bajaj@ices.utexas.edu*

ABSTRACT

We present an efficient G^1 surface reconstruction scheme for complex solid models used in FE simulations. A novel technique based on low geometric degree (biquartic) polynomial interpolation is proposed to construct a smooth surface on arbitrary unstructured (irregular) rectangular meshes. A suitable parametric representation of surface as well as local control of individual rectangular patches is achieved via simultaneous surface fitting of a curve network with corresponding cubic normals. Necessary compatibility conditions are formulated, and proved to satisfy the tangent plane continuity and vertex enclosure constraints.

Keywords: G^1 continuous, compatibility conditions, curve network, Cross Boundary Derivatives

1. INTRODUCTION

The success of high accuracy Finite Element (FE) simulations depends greatly on a precise representation of the complex geometry. In hp finite element methods, preserving the convergence rate for problems over curved domains requires that a curvilinear mesh geometry representation be used [1]. The present work is primarily motivated by an application of hp methods to simulate the absorption and diffraction of EM waves in the human head. In previous work, we interfaced the Geometric Modeling Package (GMP) with a geometric data to obtain the connectivity information, and constructed a 3D piecewise trilinear model of the human head [2]. The geometric data is generated from MRI scans by extracting adaptive meshes directly from volumetric imaging data, using a top-down octree subdivision coupled with the dual contouring method [3][4]. As a result, the head model is represented in terms of *vertex normal pair* [5], which

is defined as vertexes with attached normals on the extracted isosurface generated by Marching Cubes algorithm (MC) [6]. The GMP, working as a foundation for a multi-block hp mesh, provides *exact* parameterizations of each geometric entities which support automatic geometry updates during mesh refinements [7]. Sizable errors are introduced into the parameter prediction when the geometric approximation is too low with respect to the polynomial order of the discretization. In addition, the geometric model needs to be smooth enough to produce a finite element mesh free of local geometric discontinuities which would create artifacts in the EM solution. The hp -adaptive method requires at least a G^1 continuous geometry reconstruction. Otherwise, the hp FE code adapts meshes to resolve the non-physical scattering of waves on edges resulting from the poor, low order geometry representation.

The term *interpolation* is used here to describe ways of fitting a curve or surface to a set of data points

or curves [8]. The proposed surface reconstruction scheme is based on a parametrized surface by implementing a local interpolation on rectangular patches, and it has the following properties:

- local control of shape,
- numerical stability,
- smoothness and continuity,
- ability to evaluate derivatives.

In a smooth surface interpolation, two main forms are widely used, parametric representations and implicit representations.

There are various successful implicit surface interpolation schemes, which provide elegant solutions to the smoothing problem at the cost of a currently non standard patch representation. Bajaj and Xu proposed an approach which models a smooth surface from a surface triangulation by implicit surface patches - *A-patches* [9, 10, 11]. Other implicit schemes include B-patches [12], and S-patches [13]. A number of methods for constructing smooth parametric surfaces have also been proposed. J. Peter pioneered the idea of surface splines [14, 15, 16, 17] (see also [18, 19]), which devises a representation that removes the regularity restrictions at the cost of creating a refined mesh of quadrilateral subcells. The refined mesh guarantees that each original vertex is surrounded by vertexes of degree four. It obeys the convex hull property [20, 21]. In parallel work, H. Prautzsch [22, 23] presents a methodology enabling the construction of bisextic spline surfaces from one control net using subdivision algorithms [24, 25].

Compared with prior fitting algorithms that do not additionally split the mesh data [14, 15], we adopt cubic boundary normals instead of linearly varying normals [26] to overcome insufficiency in degenerated cases. In addition, we use a *polynomial* basis instead of rational terms [27] to guarantee regularity at vertexes. Compared to other more cumbersome G^1 methods, which are summarized in [28] and limited to triangular patches, the proposed scheme is based on a direct and efficient explicit parametric representation of rectangular patches. In particular, we focus on an arbitrary *unstructured* surface mesh, i.e., there is no restriction on the number of cells meeting at a mesh point or the number of edges adjacent to a mesh cell. This scheme has been implemented within the GMP, fitting into a general class of both explicit and implicit parameterizations.

This paper is structured as follows: Section 2.1 establishes the compatibility conditions for the curve network, and presents the theoretical analysis of adopting Hermite curves and cubic normals. Section 2.2

elaborates on the processes of interpolating G^1 biquarctic rectangular patches with twist vector compatibility conditions. Section 3 demonstrates the effectiveness of the scheme in the modeling of a human head. Section 4 summarizes and proposes future work.

2. THE CONSTRUCTION

The resulting surface must form a G^1 manifold where the patches join with G^1 continuity. Two rectangular patches \mathbf{X}_1 and \mathbf{X}_2 are G^1 compatible if and only if the normal to surface \mathbf{X}_1 is well defined (non-vanishing) and agrees with the normal of \mathbf{X}_2 at each point of the edged shared by the two patches, the so called *oriented tangent plane continuity*. Even if the curve network can be embedded into a G^1 manifold then there does not necessarily exists a polynomial solution for the above interpolation problem. The issue is related to the so called *twist incompatibility* or *vertex enclosure problem* [29, 5, 30]. The proposed methodology eliminates the above deficiencies by generating a polynomial curve network that satisfies the twist compatibility conditions. The methodology involves in two steps,

Step 1: Construction of a curve network. We construct admissible parametric curves $\xi \in [0, 1] \rightarrow \mathbf{X}_{c_i}(\xi) \in \mathbb{R}^3$, which are G^1 continuous at the vertexes. Tangent plane continuity is achieved by using an alternative sufficient constraint that forces the mesh curves to interpolate vertex data $\mathbf{p}_i, \mathbf{n}_i$ while having compatible normals $\xi \in [0, 1] \rightarrow \mathbf{N}_{c_i}(\xi) \in \mathbb{R}^3$ specified at each point on the boundary of a rectangular patch, i.e., along the mesh curves.

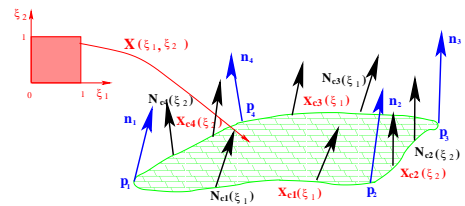


Figure 1: Interpolation of a rectangular patch

Step 2: G^1 surface fitting. We interpolate between curves of the network obtained in Step 1 using a smooth parametrized surface, by implementing an algorithm for local interpolation of rectangular patches, see Fig.1. A rectangular patch is the image of a bivariate polynomial \mathbf{X} parametrized with parameters $\xi = (\xi_1, \xi_2)$ restricted to a standard domain, $\xi \in [0, 1]^2 \rightarrow \mathbf{X} \in \mathbb{R}^3$.

2.1 Curve Network Construction

The necessary and sufficient compatibility conditions for a curve should guarantee the G^1 smoothness as well as conforming to boundaries.

DEFINITION 1 Let $\mathbf{X}_c(\xi)$ be a curve parametrization with two vertex-normal pairs $(\mathbf{p}_1, \mathbf{n}_1)$ and $(\mathbf{p}_2, \mathbf{n}_2)$, Then, its G^1 compatibility conditions are defined as: $\mathbf{X}_c(0) = \mathbf{p}_1$, $\mathbf{X}'_c(0) \cdot \mathbf{n}_1 = 0$; $\mathbf{X}_c(1) = \mathbf{p}_2$, $\mathbf{X}'_c(1) \cdot \mathbf{n}_2 = 0$. The second and fourth terms are also called essential boundary conditions. ■

Cubic curves are commonly used in graphics because it avoids using high-degree polynomials while minimizing the wiggles. The use of cubic curve can also be justified by formulating an optimization problem, seeking the solution to the following variational problem: Given two vertex-normal pairs $(\mathbf{p}_1, \mathbf{n}_1)$ and $(\mathbf{p}_2, \mathbf{n}_2)$, find a curve parametrization $\mathbf{X}_c : [0, 1] \rightarrow \mathbb{R}^3$ which satisfies G^1 compatibility conditions, and minimizes the mean (linearized) curvature,

$$I = \int_0^1 |\mathbf{X}''_c(\xi)|^2 d\xi \rightarrow \min. \quad (1)$$

The problem can be stated formally in space $\mathbf{H}^2(0, 1)$, and has a unique solution which satisfies the variational statement (equivalent to the minimization problem). For every parametrization, test function $\delta\mathbf{X}_c$ satisfying homogeneous essential boundary conditions. Integration by parts leads to

$$\int_0^1 \mathbf{X}''_c \delta\mathbf{X}_c d\xi = \int_0^1 \mathbf{X}_c^{IV} \delta\mathbf{X}_c d\xi + \mathbf{X}''_c \delta\mathbf{X}'_c|_0^1 = 0 \quad (2)$$

Restricting ourselves first to test functions that vanish on the boundary along with their first order derivatives, we get

$$\mathbf{X}_c^{IV} = 0. \quad (3)$$

This implies $\mathbf{X}_c \in \mathbf{P}^3$. The Hermite interpolation allows us to define a cubic curve segment in terms of its given endpoint vertex-normal pairs,

$$\mathbf{X}_c(\xi) = \psi_1(\xi)\mathbf{p}_1 + \psi_2(\xi)\mathbf{p}_2 + \psi_3(\xi)\mathbf{t}_1 + \psi_4(\xi)\mathbf{t}_2. \quad (4)$$

where $\psi_i \in \mathbf{P}^3$ are the standard Hermite Basis Functions, see Fig 2.

The osculating plane of the curve is spanned by the unit tangent vector $\hat{\mathbf{t}}(\xi) = \frac{\mathbf{X}'_c(\xi)}{|\mathbf{X}'_c(\xi)|}$ and the unit principal normal $\hat{\mathbf{n}}(\xi) = \hat{\mathbf{b}}(\xi) \times \hat{\mathbf{t}}(\xi)$, where $\hat{\mathbf{b}}(\xi) = \frac{\mathbf{X}'_c(\xi) \times \mathbf{X}''_c(\xi)}{|\mathbf{X}'_c(\xi) \times \mathbf{X}''_c(\xi)|}$ is the unit binormal. Decomposing $\mathbf{X}''_c(1)$ and $\delta\mathbf{X}'_c(1)$ into osculating plane, we reduce the second term in (2) to,

$$(\mathbf{X}''_c(1) \cdot \hat{\mathbf{n}})(\delta\mathbf{X}'_c(1) \cdot \hat{\mathbf{n}}) + (\mathbf{X}''_c(1) \cdot \hat{\mathbf{t}})(\delta\mathbf{X}'_c(1) \cdot \hat{\mathbf{t}}) = 0.$$

This, together with essential conditions for the test function, implies $\mathbf{X}''_c(1) \cdot \hat{\mathbf{t}} = 0$.

DEFINITION 2 Let curve parameterization $\mathbf{X}_c(\xi)$ satisfy the variational statement in (2). Then, the natural boundary conditions are defined as: $\mathbf{X}''_c(0) = \lambda_1 \mathbf{n}_1$; $\mathbf{X}''_c(1) = \lambda_2 \mathbf{n}_2$, where λ_1, λ_2 are two unknown scalars. ■

The essential boundary conditions and natural boundary conditions above yield a linear system of 8×8 equations that can be solved for the components of \mathbf{t}_1 , \mathbf{t}_2 , and constants λ_1 and λ_2 .

Lemma 1 The solution to a minimization problem of a curve $\mathbf{X}_c(\xi)$ with two vertex-normal-pairs $(\mathbf{p}_1, \mathbf{n}_1)$ and $(\mathbf{p}_2, \mathbf{n}_2)$, is a uniquely defined cubic curve whose second derivative w.r.t. ξ is parallel to normals at the endpoints. ■

The cubic curve may degenerate to a lower order polynomial. In the case of a straight line segment, $\mathbf{X}_c(\xi) \in \mathbf{P}^1$, the second derivatives of the curve vanish. Natural boundary conditions can now be solved as $\mathbf{t}_1 = \mathbf{t}_2 = \mathbf{p}_2 - \mathbf{p}_1$. In this degenerated case, the two vertex-normal-pairs must satisfy the compatibility conditions,

$$\mathbf{n}_1 \times \mathbf{n}_2 = \mathbf{n}_1 \cdot (\mathbf{p}_2 - \mathbf{p}_1) = 0. \quad (5)$$

Assume now that the cubic curve degenerates to a second order polynomial $\mathbf{X}_c(\xi) \in \mathbf{P}^2$. The vector coefficient corresponding to the third order term vanishes, and the second derivative of the curve is a constant different from zero. This implies condition (5).

THEOREM 1 The curve which satisfies minimization problem in (1), with two vertex-normal-pairs $(\mathbf{p}_1, \mathbf{n}_1)$ and $(\mathbf{p}_2, \mathbf{n}_2)$, can only degenerate to a line segment. ■

Instead of using common cross derivative functions [27, 17], we adopt independent normal function $\mathbf{N}_c(\xi)$ along the curve. Biquartic surface functions $\mathbf{X}(\xi_1, \xi_2) \in \mathbf{Q}^{(4,4)}$ involve linear combinations of twenty five monomials in ξ_1 and ξ_2 . The scalar-valued interpolation involves tensor products of five one dimensional shape functions, the Hermite basis $\psi_i(\xi)$, $i = 1, \dots, 4$ and a fifth bubble function $\psi_5(\xi) = \xi^2(1 - \xi)^2$, illustrated in Fig.2.

The order of the surface interpolation introduces four additional edge shape functions which result in a total of $(4 + 4) \times 3 = 24$ scalar unknowns to satisfy the tangent plane continuity. The *Cross Boundary Derivatives* (CBD), which is a fourth order polynomial $\mathbf{B} \in \mathbf{P}^4$, should be perpendicular to normal function

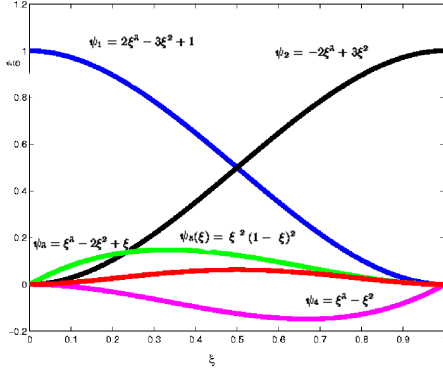


Figure 2: Five basis functions $\psi_i(\xi)$

\mathbf{N} on each of the four edges, i.e., $\mathbf{Q} = \mathbf{N}_c \cdot \mathbf{B} \equiv 0$. For an n^{th} degree polynomial fitting a curve with $n+1$ points and $\mathbf{Q} \in \mathbf{P}^7$, the maximum polynomial order of $\mathbf{N}_c(\xi)$ is three, $\mathbf{N}_c \in \mathbf{P}^3$. The normal along the curve can be written as:

$$\mathbf{N}_c(\xi) = \mathbf{n}_1\psi_1(\xi) + \mathbf{n}_2\psi_2(\xi) + \mathbf{b}_1\psi_3(\xi) + \mathbf{b}_2\psi_4(\xi), \quad (6)$$

where $\mathbf{b}_1, \mathbf{b}_2$ are two unknown vector coefficients.

DEFINITION 3 Let $\mathbf{N}_c(\xi)$ be the cubic normal along curve $\mathbf{X}_c(\xi)$, then the G^1 compatibility conditions for \mathbf{N}_c are $F(\xi) = \mathbf{X}'_c(\xi) \cdot \mathbf{N}_c(\xi) \equiv 0$. ■

As the $F(\xi) \in \mathbf{P}^5$, the above G^1 compatibility condition is equivalent to enforcing

$$\begin{aligned} F(0) = F(1) &= 0, \\ \mathbf{X}'(0) \cdot \mathbf{N}'(0) &= -\lambda_1 \|\mathbf{n}_1\|^2 \\ \mathbf{X}'(1) \cdot \mathbf{N}'(1) &= -\lambda_2 \|\mathbf{n}_2\|^2 \\ F(1/3) = F(2/3) &= 0. \end{aligned} \quad (7)$$

The first equation has already been satisfied. The second and third equations come from the natural boundary conditions.

In the case of a regular parametric surface $\mathbf{X}(\xi_1, \xi_2)$, $\frac{\partial^2 \mathbf{X}}{\partial \xi_i \partial \xi_j} \cdot \mathbf{N}$ are the so called coefficient functions of the second fundamental form. From the G^1 compatibility conditions for \mathbf{N}_c , on the boundary of the rectangular patch we have

$$\frac{\partial^2 \mathbf{X}}{\partial \xi_i \partial \xi_j} \cdot \mathbf{N} = -\frac{\partial \mathbf{X}}{\partial \xi_i} \cdot \frac{\partial \mathbf{N}}{\partial \xi_j}. \quad (8)$$

For any C^2 -parameterization, includes the biquartic parameterization under construction, the second order mixed derivative do not depend upon the order of differentiation. This implies the following necessary twist compatibility condition.

DEFINITION 4 A surface patch $\mathbf{X}(\xi_1, \xi_2)$ has compatible twist vectors at each vertex if any of the two normals $\mathbf{N}_{c_i}, \mathbf{N}_{c_j}$ on curves $\mathbf{X}_{c_i}, \mathbf{X}_{c_j}$ meeting at one vertex satisfy the twist compatibility condition: $\mathbf{N}'_{c_i} \cdot \mathbf{X}'_{c_j} = \mathbf{N}'_{c_j} \cdot \mathbf{X}'_{c_i}$ at that point. [5] ■

If the curve network has M curves, the twist compatibility condition gives us $2M$ scalar equations to be satisfied. Along with the $4M$ equations in (7), we obtain a linear global system in matrix form,

$$\mathbf{A}\mathbf{x} = \mathbf{d} \quad (9)$$

where \mathbf{A} is a $6M \times 6M$ square matrix of coefficients; \mathbf{x} is a vector of unknown degree of freedom (d.o.f) in terms of six unknown components of $\mathbf{b}_1, \mathbf{b}_2$ for each normal; \mathbf{d} is a known right-hand side vector. The matrix \mathbf{A} may degenerate to a singular matrix. It is for this reason, that we can not employ standard Gaussian elimination, and use *Singular Value Decomposition* (SVD) techniques to minimize the distance to \mathbf{d} in the least square sense [31, 32, 33].

Let's study the uniformly stability for an ill-conditioned situation deals with a cubic curve degenerating into a straight line segment in (5). Vanishing terms in (7) results in a singular matrix \mathbf{A} .

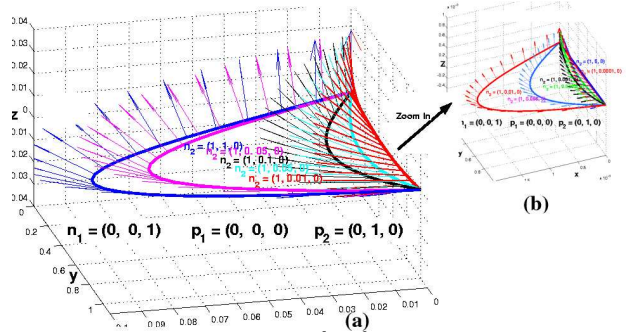


Figure 3: Stability of degenerated case for a curve with corresponding normals

The geometric data for the limit case are: $\mathbf{n}_1 = (0, 0, 1)$, $\mathbf{n}_2 = (1, 0, 0)$ and $\mathbf{p}_1 = (0, 0, 0)$, $\mathbf{p}_2 = (0, 1, 0)$. Using SVD, we study the behavior of the matrix \mathbf{A} as $\mathbf{n}_2 \rightarrow (0, 0, 1)$. We use the curve reconstruction routine, with data $\mathbf{n}_2 = (0, 1.0d - k, 1)$, $k = 0, 1, \dots, 15$. The code delivers uniformly stable results converging to the limit case. Fig. 3(a) shows the results of the curve reconstruction for values \mathbf{n}_2 varying from $(0, 1, 1)$ to $(0, 0.01, 1)$ (the red curve), then we use different scales to illustrate the convergence property in 3(b) from $(0, 0.01, 1)$ to $(0, 0, 1)$.

2.2 G^1 surface fitting

A general biquartic rectangular patch $\mathbf{X}(\xi_1, \xi_2) \in \mathcal{Q}^{(4,4)}$ can be written as the sum of vertex nodes contributions \mathbf{X}_v , mid-edge nodes contributions \mathbf{X}_e , and middle node contribution \mathbf{X}_s ,

$$\mathbf{X}(\xi_1, \xi_2) = \mathbf{X}_v(\xi_1, \xi_2) + \mathbf{X}_e(\xi_1, \xi_2) + \mathbf{X}_s(\xi_1, \xi_2). \quad (10)$$

The polynomial interpolation automatically guarantees the twist compatibility conditions at each of the vertexes.

DEFINITION 5 Let parametrization $\mathbf{X}(\xi_1, \xi_2)$ be a surface interpolation on a curve network patch with edge and normal functions $\mathbf{X}_{c_i}, \mathbf{N}_{c_i}, i = 1, \dots, 4$. The C^0 compatibility conditions are

$$\begin{aligned} (1) \mathbf{X}(\xi_1, 0) &= \mathbf{X}_{c_1}(\xi_1); & (2) \mathbf{X}(1, \xi_2) &= \mathbf{X}_{c_2}(\xi_2); \\ (3) \mathbf{X}(\xi_1, 1) &= \mathbf{X}_{c_3}(\xi_1); & (4) \mathbf{X}(0, \xi_2) &= \mathbf{X}_{c_4}(\xi_2), \end{aligned}$$

and its G^1 compatibility conditions are:

$$\begin{aligned} \frac{\partial \mathbf{X}}{\partial \xi_2}(\xi_1, 0) \cdot \mathbf{N}_{c_1}(\xi_1) &= \frac{\partial \mathbf{X}}{\partial \xi_1}(1, \xi_2) \cdot \mathbf{N}_{c_2}(\xi_2) = \\ \frac{\partial \mathbf{X}}{\partial \xi_2}(\xi_1, 1) \cdot \mathbf{N}_{c_3}(\xi_1) &= \frac{\partial \mathbf{X}}{\partial \xi_1}(0, \xi_2) \cdot \mathbf{N}_{c_4}(\xi_2) = 0. \end{aligned}$$

where $\frac{\partial \mathbf{X}}{\partial \xi_i}, i = 1, 2$ are the CBDs. \blacksquare

The $\mathbf{X}_s(\xi_1, \xi_2)$ in (10) can be written as,

$$\mathbf{X}_s(\xi_1, \xi_2) = \mathbf{s} \phi_s(\xi_1, \xi_2), \quad (11)$$

where \mathbf{s} is a vector coefficient for the middle node contribution, and ϕ_s is the corresponding face shape function, see Fig.4,

$$\phi_s = \psi_5(\xi_1) \psi_5(\xi_2). \quad (12)$$

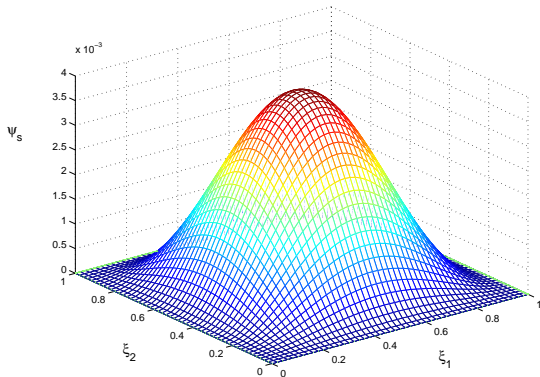


Figure 4: Face shape function ϕ_s

Note that the term $\phi_s(\xi_1, \xi_2)$ vanishes along all four edges. In other words, \mathbf{X}_s does not affect the behavior of $\mathbf{X}(\xi_1, \xi_2)$ on the boundary. On the other side,

the first two contributions in (10) are uniquely determined by the boundary data - edge functions \mathbf{X}_{c_i} and normals \mathbf{N}_{c_i} . This results in a two step procedure:

Step1: Construct a G^1 surface parameterization $\mathbf{X}^*(\xi_1, \xi_2) = \mathbf{X}_v(\xi_1, \xi_2) + \mathbf{X}_e(\xi_1, \xi_2)$ interpolating the boundary data,

Step2: Determine vector \mathbf{s} in (11) using a minimum energy principle.

2.2.1 Vertex Nodes and Mid-Edge Nodes Contributions

The $\mathbf{X}_v(\xi_1, \xi_2)$ in (10) is a standard bicubic Hermite surface interpolant $\mathbf{X}_v \in \mathcal{Q}^{(3,3)}$. It involves only vertex data and can be expressed as,

$$\begin{aligned} \mathbf{X}_v(\xi_1, \xi_2) &= \sum_{i=1}^4 \mathbf{p}_i \phi_{vi}(\xi_1, \xi_2) + \sum_{j=1}^2 \sum_{i=1}^4 \mathbf{t}_i^j \phi_{tij}(\xi_1, \xi_2) \\ &+ \sum_{i=1}^4 \mathbf{c}_i \phi_{vi}(\xi_1, \xi_2). \end{aligned} \quad (13)$$

Here

- \mathbf{p}_i denote the position vectors for each of the four vertexes i .
- ϕ_{vi} are the corresponding bicubic vertex shape functions, listed in Table 1.

Vertex number i	$\phi_{vi}(\xi_1, \xi_2)$
1	$\psi_1(\xi_1) \psi_1(\xi_2)$
2	$\psi_2(\xi_1) \psi_1(\xi_2)$
3	$\psi_2(\xi_1) \psi_2(\xi_2)$
4	$\psi_1(\xi_1) \psi_2(\xi_2)$

Table 1: The shape functions for position vector

- \mathbf{t}_i^j are eight tangent vectors, where $i = 1, \dots, 4$ is the vertex number, and $j = 1, 2$ is the index of ξ_j . For any rectangular patch, the eight tangent vectors are obtained from the curve functions \mathbf{X}_{c_i} .
- ϕ_{tij} are the corresponding shape functions for tangent vectors at vertex i in terms of ξ_j , listed in Table 2.

Vertex number i	$\phi_{ti1}(\xi_1, \xi_2)$	$\phi_{ti2}(\xi_1, \xi_2)$
1	$\psi_3(\xi_1) \psi_1(\xi_2)$	$\psi_1(\xi_1) \psi_3(\xi_2)$
2	$\psi_4(\xi_1) \psi_1(\xi_2)$	$\psi_2(\xi_1) \psi_3(\xi_2)$
3	$\psi_4(\xi_1) \psi_2(\xi_2)$	$\psi_2(\xi_1) \psi_4(\xi_2)$
4	$\psi_3(\xi_1) \psi_2(\xi_2)$	$\psi_1(\xi_1) \psi_4(\xi_2)$

Table 2: The shape functions for tangent vectors

- \mathbf{c}_i are the four unknown *twist vectors* (mixed derivatives) at each vertex i .
- ϕ_{vi} are the bicubic shape corresponding to each twist vectors, see Table 3.

Vertex number i	$\phi_{ci}(\xi_1, \xi_2)$
1	$\psi_3(\xi_1)\psi_3(\xi_2)$
2	$\psi_4(\xi_1)\psi_3(\xi_2)$
3	$\psi_4(\xi_1)\psi_4(\xi_2)$
4	$\psi_3(\xi_1)\psi_4(\xi_2)$

Table 3: The shape functions for the twist vectors

$\mathbf{X}_e(\xi_1, \xi_2)$ in (10) denotes the mid-edge nodes contributions,

$$\mathbf{X}_e(\xi_1, \xi_2) = \sum_{j=1}^2 \sum_{i=1}^4 \mathbf{e}_{ij} \phi_{eij}(\xi_1, \xi_2), \quad (14)$$

where \mathbf{e}_{ij} are eight vector coefficients to be determined, two per edge; ϕ_{eij} are the corresponding shape functions, see Table 4.

Edge number i	$\phi_{ei1}(\xi_1, \xi_2)$	$\phi_{ei2}(\xi_1, \xi_2)$
1	$\psi_5(\xi_1)\psi_3(\xi_2)$	$\psi_5(\xi_1)\psi_1(\xi_2)$
2	$\psi_4(\xi_1)\psi_5(\xi_2)$	$\psi_2(\xi_1)\psi_5(\xi_2)$
3	$\psi_5(\xi_1)\psi_4(\xi_2)$	$\psi_5(\xi_1)\psi_2(\xi_2)$
4	$\psi_3(\xi_1)\psi_5(\xi_2)$	$\psi_1(\xi_1)\psi_5(\xi_2)$

Table 4: The shape functions for edges

The C^0 compatibility conditions and the fact that the curves have been reconstructed using cubic polynomials only, $\mathbf{X}_c(\xi) \in \mathbf{P}^3$, imply that contributions corresponding to last four shape functions $\phi_{ei2}(\xi_1, \xi_2)$ must simply vanish, i.e., $\mathbf{e}_{i2} = 0, i = 1, \dots, 4$. Note that the condition does not apply to the contributions of the first four shape functions $\phi_{ei1}(\xi_1, \xi_2)$ which automatically vanish on the patch boundary and contribute only with non-zero normals.

Lemma 2 *The mid-edge node has no contribution to the mixed derivatives at each vertex of the biquartic rectangular patch.* ■

The G^1 Compatibility Conditions require the knowledge of CBDs along the boundary. The CBDs have a crucial effect on the shape of the constructed patches; they allow for the patches to effectively reflect the variation of the normals \mathbf{N}_{c_i} . The CBD at any point on the patch boundary is perpendicular to both the corresponding normal and the tangent vectors. Given the reference coordinates (ξ_1, ξ_2) of a point on the rectangular patch, we first identify four corresponding points on the patch edges with coordinates $(\xi_1, 0), (1, \xi_2), (\xi_1, 1), (0, \xi_2)$.

Note that CBDs are fourth order polynomials along the edges $\frac{\partial \mathbf{X}^*}{\partial \xi_i} \in \mathbf{P}^4$ and the normals along the curve are third order polynomials $\mathbf{N}_c \in \mathbf{P}^3$. With $\xi_1 = \xi_2 = \xi$, the G^1 compatibility conditions can be expressed as a system of equations,

$$\begin{aligned} Q(\xi) &= \frac{\partial \mathbf{X}_v}{\partial \xi_i}(\xi) \cdot \mathbf{N}_c(\xi) + \frac{\partial \mathbf{X}_e}{\partial \xi_i}(\xi) \cdot \mathbf{N}_c(\xi) \\ &= Q_c + Q_t + Q_e = 0, \end{aligned} \quad (15)$$

where Q_c and Q_e are functions in terms of four unknown twist vectors \mathbf{c}_i and four unknown vector edge coefficients \mathbf{e}_i , respectively. We have,

$$Q_c = \begin{bmatrix} (\mathbf{c}_1 \cdot \mathbf{N}_{c_1}(\xi)) & (\mathbf{c}_2 \cdot \mathbf{N}_{c_1}(\xi)) \\ (\mathbf{c}_2 \cdot \mathbf{N}_{c_2}(\xi)) & (\mathbf{c}_3 \cdot \mathbf{N}_{c_2}(\xi)) \\ (\mathbf{c}_4 \cdot \mathbf{N}_{c_3}(\xi)) & (\mathbf{c}_3 \cdot \mathbf{N}_{c_3}(\xi)) \\ (\mathbf{c}_1 \cdot \mathbf{N}_{c_4}(\xi)) & (\mathbf{c}_4 \cdot \mathbf{N}_{c_4}(\xi)) \end{bmatrix} [\psi_3(\xi) \ \psi_4(\xi)]^T,$$

and,

$$Q_e = \begin{bmatrix} (\mathbf{e}_1 \cdot \mathbf{N}_{c_1}(\xi)) \\ (\mathbf{e}_2 \cdot \mathbf{N}_{c_2}(\xi)) \\ (\mathbf{e}_3 \cdot \mathbf{N}_{c_3}(\xi)) \\ (\mathbf{e}_4 \cdot \mathbf{N}_{c_4}(\xi)) \end{bmatrix} \psi_5(\xi). \quad (16)$$

Q_t is a matrix prescribed in terms of tangent vectors \mathbf{t}_j^i ,

$$Q_t = \begin{bmatrix} (\mathbf{t}_1^2 \cdot \mathbf{N}_{c_1}(\xi)) & (\mathbf{t}_2^2 \cdot \mathbf{N}_{c_1}(\xi)) \\ (\mathbf{t}_2^1 \cdot \mathbf{N}_{c_2}(\xi)) & (\mathbf{t}_3^1 \cdot \mathbf{N}_{c_2}(\xi)) \\ (\mathbf{t}_4^2 \cdot \mathbf{N}_{c_3}(\xi)) & (\mathbf{t}_3^2 \cdot \mathbf{N}_{c_3}(\xi)) \\ (\mathbf{t}_1^1 \cdot \mathbf{N}_{c_4}(\xi)) & (\mathbf{t}_4^1 \cdot \mathbf{N}_{c_4}(\xi)) \end{bmatrix} [\psi_1(\xi) \ \psi_2(\xi)]^T.$$

As $Q(\xi)$ is a seventh order polynomial $Q(\xi) \in \mathcal{P}^7$, vanishing at the endpoints of the edge, enforcing G^1 compatibility condition is equivalent to enforcing,

$$Q\left(\frac{i}{N}\right) = 0, \quad i = 1, N-1, \quad (17)$$

with $N = 7$. Solving a system of $(7-1) \times 4 = 24$ equations, we get values of eight vector coefficients $\mathbf{c}_i, \mathbf{e}_i, i = 1, \dots, 4$.

2.2.2 Middle node Contribution

Mathematical formulation of any boundary value problem consists of a differential equation and boundary conditions. The connection between transfinite interpolation and the boundary value problems is explicit in the last section. In our case, we exactly interpolate the prescribed boundary conditions. However, the behavior of the interpolant away from the boundaries is quite arbitrary. Thus, the solution of a boundary value problem can be viewed as the construction of a function that extends the boundary conditions into the domain, with differential equations playing the role of a constraining or smoothing operator.

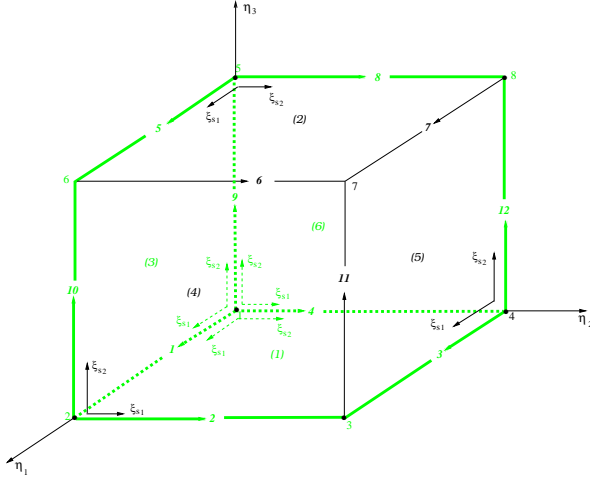


Figure 5: A hexahedron in the reference frame

The interpolation problem has no unique solution; there are infinitely many functions interpolating any given data. An unique construction can be established by putting additional constraints on the interpolant. Often such constraints appear as the minimization of some quantity. Many interpolation schemes use minimization of energy [34] as a means for controlling the shape of the interpolant,

$$I = \int_{\Omega} (\Delta \mathbf{X}(\xi_1, \xi_2))^2 d\Omega \rightarrow \min, \quad (18)$$

where $\Delta = \frac{\partial^2}{\partial \xi_1^2} + \frac{\partial}{\partial \xi_1} \frac{\partial}{\partial \xi_2} + \frac{\partial^2}{\partial \xi_2^2}$, Ω is the rectangular reference domain, and

$$\mathbf{X}(\xi_1, \xi_2) = \mathbf{X}^*(\xi_1, \xi_2) + \mathbf{s}\phi_s(\xi_1, \xi_2), \quad (19)$$

with the first term $\mathbf{X}^*(\xi_1, \xi_2)$ interpolating the boundary conditions given in equation (10); $\mathbf{s} = (s^{(1)}, s^{(2)}, s^{(3)})$ is the vector unknown for the middle node; ϕ_i are shape function described before. The

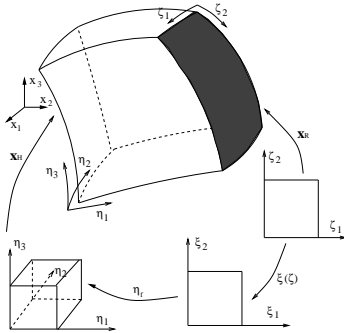


Figure 6: Compatibility of parameterizations for a hexahedron

value of the coefficient \mathbf{s} is obtained by minimizing (18). Upon differentiating (19) with respect to

$s_k, k = 1, \dots, 3$, we construct and solve a system of three linear equations for components of \mathbf{s} ,

$$\frac{\partial I}{\partial s_k} = \int_{\Omega} \sum_{k=1}^3 (\Delta \mathbf{X}^{*(k)} + s_k \Delta \phi_i) \Delta \phi_i = 0. \quad (20)$$

3. MODELING OF A 3D G^1 HUMAN HEAD FOR HP FE SIMULATION

The discussed G^1 continuous geometry reconstruction technique has been applied to model the geometry of a human head, necessary for high accuracy 3D hp FE simulation. The implementation has been done within our Geometrical Modeling Package (GMP) [2] interfaced with software LBIE - Mesh Level Set Boundary and Interior-Exterior Mesher [3][4], developed at Center for Computational Visualization (CCV) at ICES. The data, obtained from an MRI scan of a human head, provides a coarse trilinear hex mesh. The minimum topological representation (hex to points connectivities) and a geometrical (normals) data is then imported into GMP, where the actual G^1 continuous geometry reconstruction takes place.

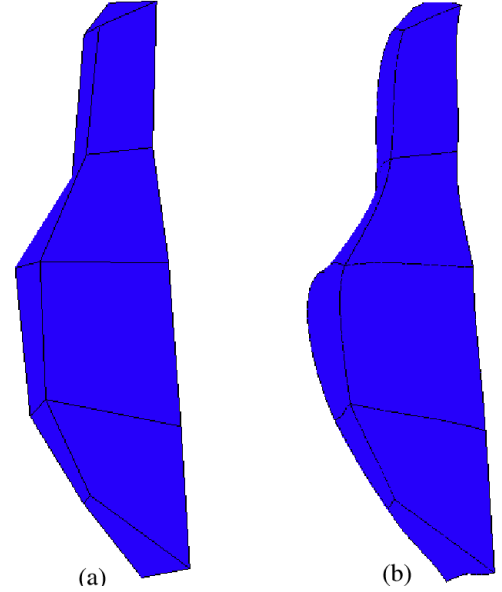


Figure 7: The nose model of the human head. (a) C^0 continuous model (b) G^1 continuous model

The use of high order FE method puts certain requirements for geometric modeling. The small size of the GMP is used to maintain a continuous interface with the adaptive codes. The GMP [7] not only supports the construction of exact parameterizations for a general class of 2D (BEM) [35] and 3D (FEM)[36] objects, but also provides the derivatives of the mappings with respect to reference coordinates. In our geometric modeling, a 2D object is represented as a union of

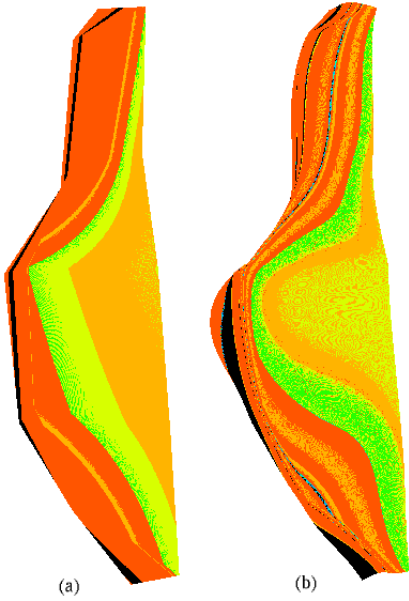


Figure 8: Color map of isophotes of the nose.(a) C^0 continuous model (b) G^1 continuous model

curvilinear triangles or rectangles, while a 3D object is represented with a FE-like mesh of curvilinear hexahedral blocks. Each of the geometric objects is identified with its corresponding parameterization. Next we divided the reference brick into subelements with corresponding order of approximation. As a result, the GMP model is used to generate so called initial FE mesh of arbitrary high order, and to support geometry updates during mesh refinements. Each of the local edges or faces in the GMP has its own global orientation, see Fig.5. Adjusting edge and face parameterizations for orientations involves transforming local edge and face coordinates into the global coordinates. We must ensure the *compatibility of parameterizations*[7], which is illustrated in Fig.6.

The construction of the human head model is based on two GMP parameterizations: *Transfinite Interpolation Rectangles* and *Transfinite Interpolation Hexahedra*, both based on the classical transfinite interpolation and linear blending functions technique [37, 38]. Using the interface, we reconstruct a curvilinear hex-mesh with a G^1 continuous representation of the surface for the 3D model. The obtained hex-mesh head model is then used to generate the actual meshes for hp-Adaptive FE simulations.

Before generating the whole human head model, we first test the scheme on some feature parts of the head, *e.g.*, the nose. Any hexahedron that constitutes a part of the nose is a special case because all its eight vertices are on the G^1 surface. The obtained 3D linear nose model in Fig. 7(a) is then reconstructed into a

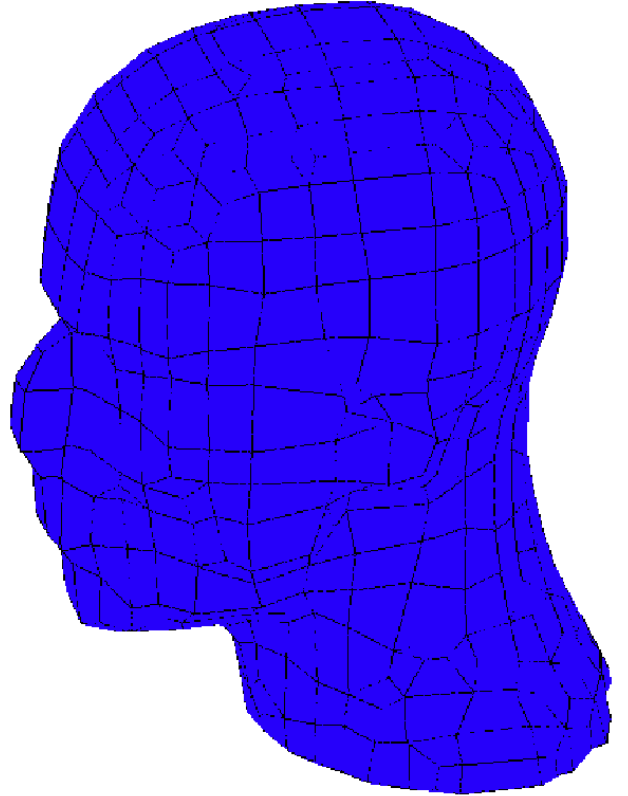


Figure 9: The head model as a union of curvilinear hexahedra

a curvilinear model, illustrated in in Fig. 7(b). Fig.8 displays the usual way of visualizing isophotes on the surface [39, 40]. The isophotes here are computed in the following way: choose a (small) interval and mark all points on the surface where the values of isophotes are in the interval. The result are not the isophotes themselves but point set on the surface which give an impression of the behavior of the isophotes. In particular we can see that point sets have varying “thickness” [41].

The entire reconstructed human head model is presented in Fig.9, which is to eventually simulate EM waves in a human head. This involves enclosing the head within a truncating sphere, and meshing the entire volume within the sphere, and the head. Special absorbing boundary conditions are imposed on the truncating sphere to model the interaction with the rest of the space. The color map of its isophotes in Fig.10 shows the smoothness of the G^1 continuous surface.

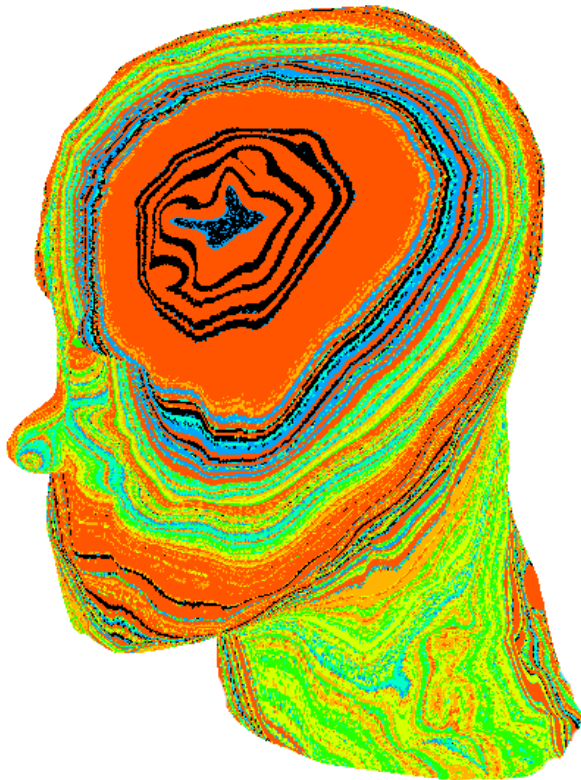


Figure 10: The color map of isophotes of the head model.

4. CONCLUSIONS AND FUTURE WORKS

The paper presents results of a preliminary study on geometric reconstruction in context of geometries reproduced from MRI scans and mesh generation for high order hp FE discretization. The presented bi-quartic scheme seems to be the lowest order G^1 continuity construction for general unstructured meshes. The polynomial parameterizations are inexpensive to compute and guarantee high regularity of parametrization necessary in FE computations. It is not clear at this point, however, how the G^1 regular parametrization will affect the convergence rates of high order methods. The important property of the presented G^1 reconstruction scheme is that it remain uniformly stable in the case of degenerated geometrical data .

Among other tasks, we intend also to collaborate with CCV on multi-resolution techniques and hierarchical geometry reconstruction schemes. At this point, the information on geometry contained in the original fine mesh reconstruction, during the coarsing stage is reduced to normals only. Ideally, the geometry reconstruction on the coarse grid should conform to the fine grid representation in a more elaborate, multi-

resolution model. We intend to address these topics in our future work.

References

- [1] Dey S., Shephard M.S., E J. "Geometry Representation Issues Associated with p-Version Finite Element Computations." *Rensselaer SCOREC report*, vol. 4, 1997
- [2] Xue D., Demkowicz L. "An Interface Between Geometrical Modeling Package(GMP) and Mesh-Based Geometry(MBG)." *ICES Report*, vol. 03, 2003
- [3] Zhang Y., Bajaj C., Sohn B.S. "Adaptive and Quality 3D Meshing from Imaging Data." *Proceedings of 8th ACM Symposium on Solid Modeling and Applications*, vol. June 16-20, 286–291, 2003
- [4] Zhang Y., Bajaj C., Sohn B.S. "3D Finite Element Meshing from Image Data." *Accepted in the special issue of Computational Methods in Applied Medhanics and Engineering on unstructural mesh generation*, 2004
- [5] Bajaj C., Lhm I. "Smooth Polyhedra using Implicit Algebraic Splines." *Computer Graphics*, pp. 79–88, July 1992
- [6] Lorensen W.E., Cline H.E. "A high resolution 3d surface construction algorithm." *In Proceedings of SIGGRAPHn*, p. 163169, 1987
- [7] Xue D., Demkowicz L. "Geometrical Modeling Package Version 2.0." *TICAM Report*, vol. 02-30, 2002
- [8] M.A.Sabin. "Transfinite Surface Interpolation." *Proceedings of a sixth conference on Mathematics of Surfaces*, 1996
- [9] Bajaj C., Chen J., Xu G. "Modeling with Cubic A-patches." *ACM Transactions on Graphics*, vol. 14, 103–133, April 1995
- [10] Bajaj C., Chen J., Xu G. "Modeling with Cubic A-patches ACM Transactions on Graphic." *14*, vol. 2, 103–133, April,(1995)
- [11] Xu G., Bajaj C., Huang H. "C1 Modeling with A-patches from Rational Trivariate Functions Computer Aided Geometric Design." *18*, vol. 3, 221–243, 2001
- [12] H.P.Seidel. "Symmetric Recursive Algorithms for Surfaces: B-patches and the De Boor Algorithm for Polynomials Over Triangles." *Constr. Approx.*, vol. 7, 257–279, 1991

- [13] C.T.Loop, T.DeRose. "Generalized B-spline Surfaces of Arbitrary Topology." *Computer Graphics*, vol. 24, 347–356, 1990
- [14] Peters J. "C1 Surface Splines." *SIAM J. of Numer. Anal.*, vol. 32-2, 645–666, 1995
- [15] Peters J. "Biquartic C1-surface Splines Over Irregular Meshes." *CAD*, Jan 95
- [16] Peters J. "Surfaces of Arbitrary Topology Constructed from Biquadratics and Bicubics." *Designing fair curves and surfaces*, vol. SIAM Publications, N. Sapidis, 1994
- [17] Peters J. "Smooth Free-form Surfaces Over Irregular Meshes Generalizing Quadratic Splines." *CAGD*, pp. 347–361, 1993
- [18] A.R.M.Piah. "Construction of Smooth Surfaces by Piecewise Tensor Product Polynomials." *CS Report*, vol. 91/04, University of Dundee, UK, 1991
- [19] O.Reif. "Biquadratic G-spline Surfaces." *Preprint 93-4*, vol. Math Ins A, University Stuttgart, 1993
- [20] M.Sabin. "Non-rectangular Surface Patches Suitable for Inclusion in a B-spline Surface." *Proceedings of Eurographics*, vol. North Holland, 57–69, 1983
- [21] T.N.T.Goodman. "Closed Surfaces Defined From Biquadratic Splines." *Constructive Approximation*, vol. 7, 149–160, 1991
- [22] Prautzsch H. "Freeform Splines." *Computer Aided Geometric Design*, vol. 14, 201–206, 1997
- [23] Bangert C., Prautzsch H. "Quadric Splines." *Computer Aided Geometric Design*, vol. Academic Press, 181–193, 1989
- [24] Prautzsch H., Umlauf G. "A G2-Subdivision Algorithm." *Geometric Modelling*, pp. 217–224, 1996
- [25] Prautzsch H., Umlauf G. "Improved Triangular Subdivision Schemes." *Computer Graphics International*, pp. 626–632, 1998
- [26] Peters J. "Local cubic and bicubic C1 surface interpolation with linearly varying boundary normal." *Computer Aided Geometric Design*, pp. 499–516, 1990
- [27] T.Hermann. "G2 interpolation of free form curve network by biquintic Gregory patches." *Computer aided geometric design*, vol. 13, 873–893, 1996
- [28] S. M., C. L. "A survey of parametric scattered data fitting using triangular interpolants." *Curve and Surface Design*, vol. SIAM, 145–172, 1992
- [29] interpolation without twist constraints S. "Computer Aided Geometric Design." *Academic Press*, vol. New York, 71–87, 1974
- [30] Peter J. "Smooth Interpolation of a Mesh of Curves." *Constructive Approximation*, vol. 7, pp.221–246, 1991
- [31] Gentle J.E. "Singular Value Factorization." *Numerical Linear Algebra for Applications in Statistics*, vol. Berlin: Springer-Verlag, 102–103, 1998
- [32] Golub G.H., Van Loan C.F. "The Singular Value Decomposition." *2.5.3 and 2.5.6 in Matrix Computations*, vol. 3rd ed. Baltimore, Johns Hopkins University Press, 70–71, 1996
- [33] Nash J.C. "The Singular-Value Decomposition and Its Use to Solve Least-Squares Problems." *Compact Numerical Methods for Computers: Linear Algebra and Function Minimisation*, vol. Bristol, England: Adam Hilger, 30–48, 1990
- [34] Hoschek J., Lasser D. "Fundamentals of Computer Aided Geometric Design." *A K Peters*, 1993
- [35] Demkowicz L. "2D hp-Adaptive Finite Element Package(2Dhp90) Version 2.0." *TICAM Report*, vol. 02-06, 2002
- [36] Demkowicz L., Pardo D., Rachowicz W. "3D hp-Adaptive Finite Element Package(2Dhp90)." *TICAM Report*, vol. 02-24, 2002
- [37] Gordon W.J., Hall C.A. "Transfinite Element Methods: Blending Function Interpolation over Arbitrary Curved Element Domains." *Numer. Math.*, vol. 21, 109–129, 1973
- [38] Gordon W.J. "Blending Function Methods of Bivariate and Multivariate Interpolation and Approximation." *SIAM J. Numer. Anal*, vol. 8, 158–177, 1971
- [39] h. H., S.Hahmann, T.Schreiber. "Surface interrogation algorithms." *Comp.Graphics and Applies*, vol. 12(5), 53–60, 1992
- [40] Poeschl T. "Detecting surface irregularities using isophotes." *Comput. Aided Geom. Design*, vol. 1(2), 163–168, 1984
- [41] Theisel H. "On Geometric Continuity of Isophotes." *Proceedings of Chamonia*, pp. 1–8, 1996